Methodology for assessing fundamental parametric roll other than the principal parametric roll

Yuta Uchida, *Osaka University,* uchida_yuta@naoe.eng.osaka-u.ac.jp
Masahiro Sakai, *Osaka University,* sakai@naoe.eng.osaka-u.ac.jp
Naoya Umeda, *Osaka University,* umeda@naoe.eng.osaka-u.ac.jp

ABSTRACT

It is desirable to establish simplified methods for estimating the fundamental parametric rolling in longitudinal waves. For the occurrence condition, a method is developed using a harmonic balance method. For the direct and simplified estimation of the amplitude, an averaging method is applied to an uncoupled nonlinear roll equation. These methods provide reasonable comparisons with the free-running model experiment of a car carrier in regular following seas, apart from harmonic rolling due to yaw-roll coupling at higher speed.

Keywords: *harmonic balance method, averaging method, direct stability assessment, vulnerability criteria, pure loss of stability*

1. INTRODUCTION

The International Maritime Organization (IMO) approved the second-generation intact stability criteria in 2020 (IMO, 2020), consisting of the level 1 and 2 vulnerability criteria and the direct stability assessment. These criteria require us to judge ship stability with different criteria depending on the stability failure modes. In the case of the direct stability assessment, the stability failure found by time-domain numerical simulation should be verified whether it is the intended failure mode or not. (IMO, 2022)

If the identified failure mode is different from the stability failure modes that the vulnerability criteria are provided, the results of direct stability assessment cannot be utilized for regulatory purposes. It is because the use of direct stability assessment without the application of vulnerability criteria should not be penalized. For avoiding such a situation, the vulnerability criteria should be developed for the remaining stability failures as soon as possible.

One of the major candidates for the remaining failure modes is the fundamental parametric rolling. As well established, parametric rolling, in general, could occur with the roll frequency being multiple of half the encounter wave frequency. However, the second generation intact stability criteria deal with only principal parametric rolling, in which the roll frequency is equal to half the encounter wave frequency, among the various parametric rolling because the principal parametric rolling is most significant. Indeed, most recently reported accidents, such as that of the C11 class containership in the North Pacific, are due to principal parametric rolling at low speed in head or following waves. On the other hand, the fundamental parametric rolling, in which the roll frequency is equal to the encounter wave frequency, could be found at higher speeds in following waves when we execute comprehensive numerical simulations. (IMO, 2022)

Therefore, we explore the possibility of vulnerability criteria for the fundamental parametric rolling, keeping a reasonable relationship with the direct stability assessment. Firstly, existing experimental data of fundamental parametric rolling is identified as a kind of direct stability assessment. Secondly, a simplified estimation method for the amplitude of fundamental parametric rolling is developed based on an averaging method applied to an uncoupled roll model. Finally, a simplified method for estimating the occurrence of fundamental rolling is developed based on a harmonic balance method.

2. MODEL EXPERIMENT

Sakai et al. (2017) executed model experiments of a pure car carrier (PCC) at the seakeeping and manoeuvring basin of the National Research Institute of Fisheries Engineering. The principal particulars of the PCC are shown in Table 1. A free-

running experiment was carried out in regular following waves with a PD autopilot, a propulsion motor and a propeller. A fibre optical gyroscope measured the roll, pitch and yaw motions, and the model trajectory was measured by a total station system so that the ship's forward velocity was precisely determined. Here the wavelength is equal to the ship length between perpendiculars, the wave steepness was 0.07, and the autopilot course was set to be 10 degrees from the wave direction towards the left-hand side. As shown in Figure 1, a typical fundamental parametric roll, in which the wave encounter period is equal to the roll period and is close to the natural roll period, was observed under the Froude number of 0.169. During one cycle, the centre of roll motion is shifted toward the starboard and the largest roll occurs whenever the ship's centre meets the wave upslope. The roll restoring moment decreases at the wave crest amidship so that the larger roll develops at the wave crest amidship than at the wave trough amidship.

Table 1: Principal particulars of the PCC

	Items	Ship	Model	
Length between perpendiculars	L_{pp}	180	3.366	[m]
He Breadth	B	32.2	0.6022	[m]
Draught	d	8.20	0.1534	[m]
Metacentric height	GM	1.266	0.02368	[m]
Natural roll period	T_φ	23.4	3.2	[s]

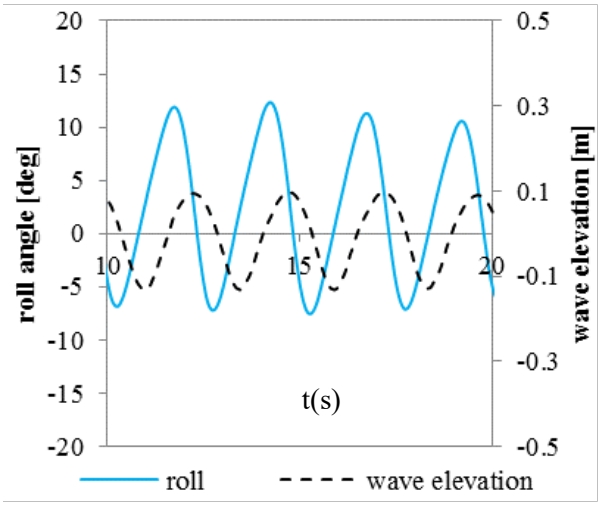

Figure 1 An example of the fundamental parametric rolling observed in the model experiment with the wave elevation at the ship centre. Here the positive wave elevation indicates the downward. (Sakai et al., 2017)

3. MATHEMATICAL MODEL

An uncoupled roll equation is used as Eq. (1) to develop the simplified estimation method.

$$\ddot{\phi} + 2\alpha\dot{\phi} + \gamma\dot{\phi}^3 + {\omega_\phi}^2(\phi + l_3\phi^3 + l_5\phi^5) + {\omega_\phi}^2\{F' + M'(k_1\cos\omega_e t + k_2\cos 2\omega_e t)\}\left(\phi - \frac{\phi^3}{\pi^2}\right) = 0 \quad (1)$$

where ϕ is the roll angle, and the dot indicates the differentiation concerning time. α and γ are linear and cubic roll damping coefficients, respectively. ω_ϕ and ω_e are the natural and encounter frequencies, respectively. F' and M' are the bias and the amplitude of GM variation in waves, respectively, as given by Eq. (2)

$$F' = \frac{GM_{ave} - GM}{GM}, \quad M' = \frac{GM_{max} - GM_{ave}}{GM} \quad (2)$$

GM_{ave} *and* GM_{max} are the average of GM in waves during one cycle and the maximum of GM, respectively. Since the GM variation in waves consists of the harmonic and subharmonic components, as shown in Figure 2. k_1 and k_2 are coefficients obtained by the Fourier series expansion.

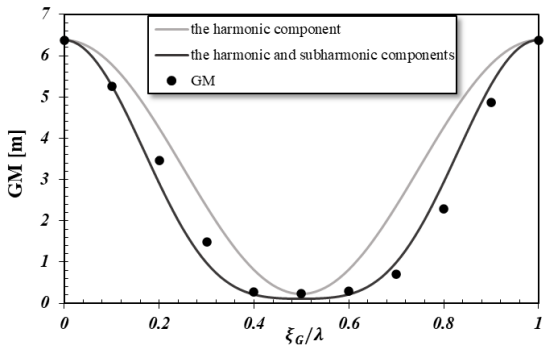

Figure 2 GM variation in waves.

4. AVERAGING METHOD

Fundamental parametric rolling has the bias, the harmonic and the second harmonic components. Thus, we assume the solution of Eq. (1) as Eq. (3) for the averaging method.

$$\phi = A_0 + A_1\cos(\hat{\omega}t - \varepsilon_1) + A_2\cos(2\hat{\omega}t - \varepsilon_2) \quad (3)$$

The assumed solution is substituted into the equation of motion. After averaging it for one cycle with $\hat{\omega} = \omega_e$, the simultaneous algebraic equation set can be obtained as shown in Appendix 1. Then,

the steady amplitudes, phases, and bias can be determined by solving it using a numerical iteration technique. These outcomes allow us to calculate the maximum roll angle during one encounter wave cycle as a function of the Froude number. The numerical results of this averaging method were plotted in Figure 3, together with the time-domain simulation results of Eq. (1) using the Runge Kutta method. The averaging method provides slightly conservative results. The difference between the averaging method and the time domain simulation is due to the super-harmonics other than the second harmonic included in Eq. (3).

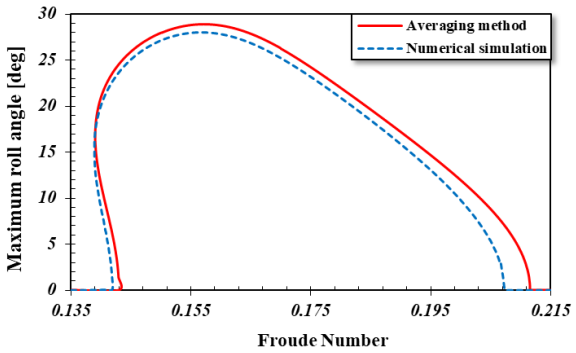

Figure 3 Maximum roll angle during one encounter wave cycle calculate by the averaging method and the time-domain simulation of Eq. (1).

Thus, it is possible to straightforwardly estimate the amplitude of fundamental parametric rolling so that the level 2 parametric rolling can be developed. Using the averaging method is advantageous for directly identifying the fundamental parametric rolling without verifying the failure mode.

5. HARMONIC BALANCE METHOD

For the harmonic balance method, we assume the periodic solution as follows:

$$\phi = A_0 + A_1 \cos\hat{\omega}t + B_1 \sin\hat{\omega}t + A_2 \cos 2\hat{\omega}t + B_2 \sin 2\hat{\omega}t \quad (4).$$

The assumed solution is substituted into the linearized version of Eq. (1). Then we put $\hat{\omega} = \omega_e$ and obtain the requirements for the coefficients of the constant terms, $\cos\omega_e t$, $\sin\omega_e t$, $\cos 2\omega_e t$, and $\sin 2\omega_e t$. They can be regarded as a simultaneous linear equation set of A_0, A_1, B_1, A_2 and B_2. The condition for the existence of a non-trivial solution set can be obtained by calculating its determinant. If it has a non-trivial solution set, the fundamental parametric rolling shall exist. Thus, the fundamental parametric rolling occurrence condition can be determined in Appendix 2. This formula calculates the range of occurrence of fundamental parametric rolling, as shown as a shaded range in Figure 4. The estimated range satisfactorily agrees with the results of the averaging method. Therefore, it can be used to develop the level 1 vulnerability criterion.

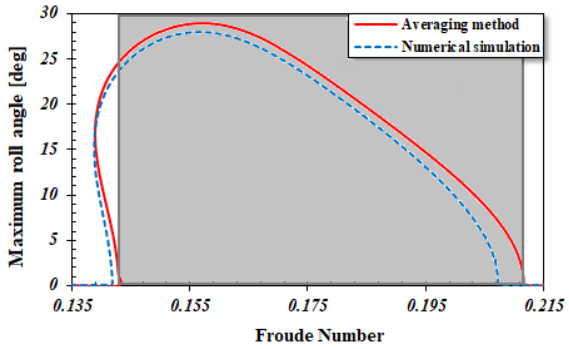

Figure 4 Range of occurrence of fundamental parametric rolling estimated by the harmonic balance method.

6. DISCUSSION

The above results are compared with the aforementioned experimental method, as shown in Figure 5. In the range of fundamental parametric rolling, the averaging method provides conservative estimates for the amplitude. On the other hand, significant rolling also exists at higher speeds outside the estimated range of fundamental parametric rolling.

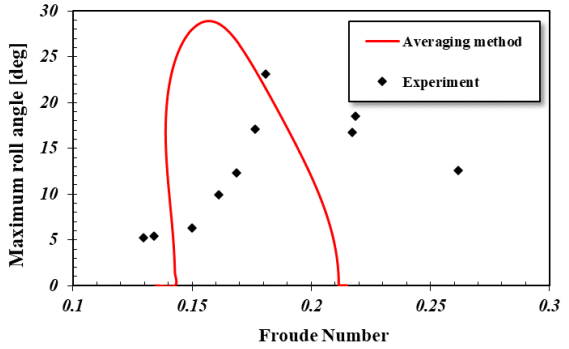

Figure 5 Comparison between the model experiment and the averaging method.

As shown in Figure 6, the measured roll motion at this higher speed region is harmonic, but the phase difference is different from the case of Figure 1. The maximum roll occurs at the wave crest amidship in place of the wave upslope. For investigating the reason, we apply the manoeuvring-based surge-sway-yaw-roll numerical model with the wave effect (Kubo et al., 2012) to this series of experiments, as

shown in Figures 7 and 8. This numerical model well agrees with the model experiment in the higher region. Thus, we can conclude that the significant role outside the estimated region for fundamental parametric rolling is not parametric rolling but yaw-roll coupling with loss of stability, which the methodology should deal with for pure loss of stability.

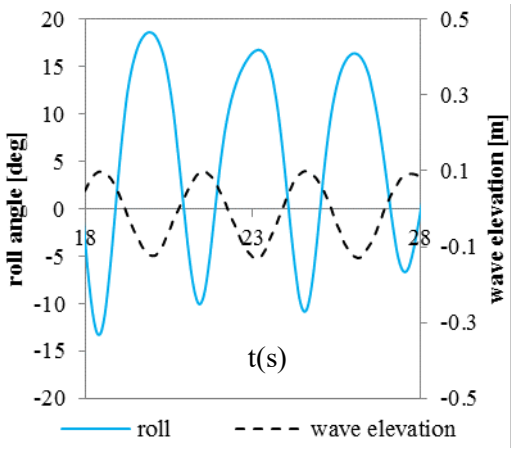

Figure 6 Measured data of roll motion in following waves at the Froude number of 0.219. (Sakai et al., 2017)

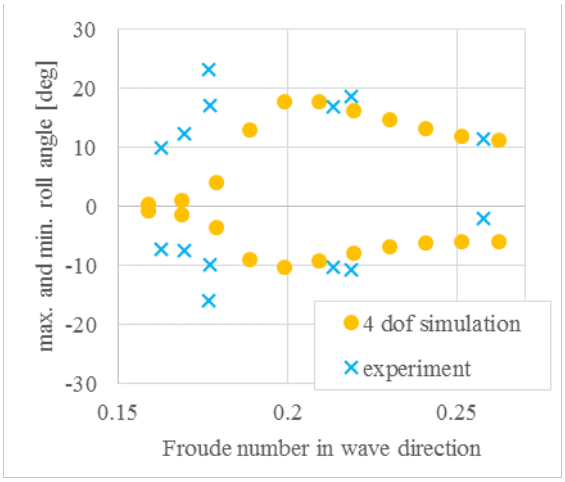

Figure 7 Maximum and minimum roll angles estimated by the manoeuvring-based simulation and model experiment (Sakai et al., 2017).

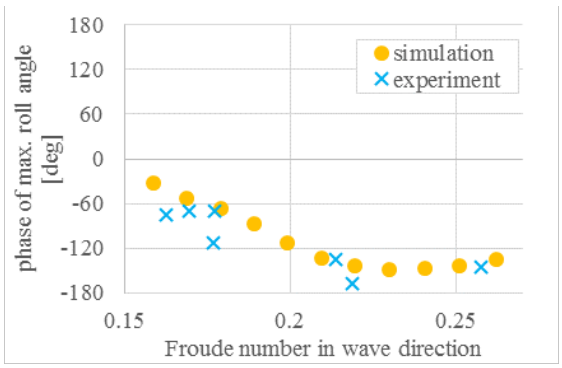

Figure 8 Phase difference of maximum roll angle to waves estimated by the manoeuvring-based simulation and model experiment (Sakai et al., 2017).

7. CONCLUSIONS

A simplified method for estimating the occurrence condition of fundamental parametric rolling is developed based on the harmonic balance method. A direct method for estimating the amplitude of fundamental parametric rolling is developed based on the averaging method. These outcomes provide reasonable comparisons with the model experiment, apart from the harmonic roll at higher speed in following waves, which is due to yaw-roll coupling with loss of the transverse stability.

ACKNOWLEDGEMENTS

This work was supported by a Grant-in-Aid for Scientific Research from the Japan Society for Promotion of Science (JSPS KAKENHI Grant Number 19H02360). It was partly carried out as a research activity of the Goal-based Stability Criteria Project of the Japan Ship Technology Research Association in the fiscal year of 2021, funded by the Nippon Foundation.

REFERENCES

IMO, 2020, "Interim Guidelines on the Second Generation Intact Stability Criteria", MSC.1/Circ.1627, pp.1-60.

IMO, 2022, "Draft MSC Circular, Explanatory Note to the Interim Guidelines on the Second Generation Intact Stability Criteria", SDC 8/18/Add.1.

Kubo, H., Umeda, N., Yamane, K. and Matsuda, A., 2012, "Pure Loss of Stability in Astern Seas –Is it Really Pure?-", the 6th Asia-Pacific Workshop on Marine Hydrodynamics, Johor, pp.307-312.

Sakai, M., Umeda, N., Terada, D., Matsuda, A., 2017, "The Relationship between Parametric Roll in Secondary Unstable Regions and Pure Loss of Stability", Conference Proceedings of Japan Society of Naval Architects and Ocean Engineers, Vol.24, pp.291-294.

Appendix 1

The parameters in Eq. (3) can be determined with the following formulae.

$$
\begin{aligned}
0 = &-\alpha A_1 - \gamma {\omega_e}^2 \left(\frac{3}{8}{A_1}^3 + 3A_1{A_2}^2\right) \\
&+ M' k_1 \sin(\varepsilon_1)\left(\frac{{\omega_\phi}^2}{\omega_e}\right)\left(\frac{1}{2\pi^2}{A_0}^3 + \frac{3}{8\pi^2}A_0{A_1}^2\right. \\
&\left.+ \frac{3}{4\pi^2}A_0{A_2}^2 - \frac{1}{2}A_0\right) \\
&+ M' k_2 \sin(2\varepsilon_1)\left(\frac{{\omega_\phi}^2}{\omega_e}\right)\left(\frac{3}{4\pi^2}{A_0}^2A_1 + \frac{1}{8\pi^2}{A_1}^3\right. \\
&\left.+ \frac{3}{8\pi^2}A_1{A_2}^2 - \frac{1}{4}A_1\right) \\
&+ M' k_2 \sin(2\varepsilon_1 - 2\varepsilon_2)\left(\frac{{\omega_\phi}^2}{\omega_e}\right)\left(\frac{3}{16\pi^2}A_1{A_2}^2\right) \\
&- \sin(4\varepsilon_1 - 2\varepsilon_2)\left(\frac{{\omega_\phi}^2}{\omega_e}\right)\left(\frac{5}{16}l_5{A_1}^3{A_2}^2\right) \\
&+ M' k_1 \sin(\varepsilon_1 - \varepsilon_2)\left(\frac{{\omega_\phi}^2}{\omega_e}\right)\left(\frac{3}{4\pi^2}{A_0}^2A_2 + \frac{3}{16\pi^2}{A_1}^2A_2\right. \\
&\left.+ \frac{3}{16\pi^2}{A_2}^3 - \frac{1}{4}A_2\right) \\
&- \sin(2\varepsilon_1 - \varepsilon_2)\left(\frac{{\omega_\phi}^2}{\omega_e}\right)\left(\frac{3}{2}l_3A_0A_1A_2 + 5l_5{A_0}^3A_1A_2\right. \\
&\left.+ \frac{5}{2}l_5A_0{A_1}^3A_2 + \frac{15}{4}l_5A_0A_1{A_2}^3 - \frac{3}{2\pi^2}F'A_0A_1A_2\right) \\
&+ M' k_1 \sin(3\varepsilon_1 - \varepsilon_2)\left(\frac{{\omega_\phi}^2}{\omega_e}\right)\left(\frac{3}{16\pi^2}{A_1}^2A_2\right)
\end{aligned}
\qquad (A.1)
$$

$$
\begin{aligned}
0 = {} & \frac{1}{2}\omega_e A_1 - \frac{1}{2}\left(\frac{\omega_\phi{}^2}{\omega_e}\right)A_1 \\
& + F'\left(\frac{\omega_\phi{}^2}{\omega_e}\right)\left(\frac{3}{2\pi^2}A_0{}^2A_1 + \frac{3}{8\pi^2}A_1{}^3 + \frac{3}{4\pi^2}A_1A_2{}^2 - \frac{1}{2}A_1\right) \\
& - l_3\left(\frac{\omega_\phi{}^2}{\omega_e}\right)\left(\frac{3}{2}A_0{}^2A_1 + \frac{3}{8}A_1{}^3 + \frac{3}{4}A_1A_2{}^2\right) \\
& - l_5\left(\frac{\omega_\phi{}^2}{\omega_e}\right)\left(\frac{5}{2}A_0{}^4A_1 + \frac{15}{4}A_0{}^2A_1{}^3 + \frac{5}{16}A_1{}^5\right. \\
& \left. + \frac{15}{2}A_0{}^2A_1A_2{}^2 + \frac{15}{8}A_1{}^3A_2{}^2 + \frac{15}{16}A_1A_2{}^4\right) \\
& + M'k_1\cos(\varepsilon_1)\left(\frac{\omega_\phi{}^2}{\omega_e}\right)\left(\frac{1}{2\pi^2}A_0{}^3 + \frac{9}{8\pi^2}A_0A_1{}^2\right. \\
& \left. + \frac{3}{4\pi^2}A_0A_2{}^2 - \frac{1}{2}A_0\right) \\
& + M'k_2\cos(2\varepsilon_1)\left(\frac{\omega_\phi{}^2}{\omega_e}\right)\left(\frac{3}{4\pi^2}A_0{}^2A_1 + \frac{1}{4\pi^2}A_1{}^3\right. \\
& \left. + \frac{3}{8\pi^2}A_1A_2{}^2 - \frac{1}{4}A_1\right) \qquad (A.2) \\
& + M'k_2\cos(2\varepsilon_1 - 2\varepsilon_2)\left(\frac{\omega_\phi{}^2}{\omega_e}\right)\left(\frac{3}{16\pi^2}A_1A_2{}^2\right) \\
& - \cos(4\varepsilon_1 - 2\varepsilon_2)\left(\frac{\omega_\phi{}^2}{\omega_e}\right)\left(\frac{5}{16}l_5A_1{}^3A_2{}^2\right) \\
& + M'k_1\cos(\varepsilon_1 - \varepsilon_2)\left(\frac{\omega_\phi{}^2}{\omega_e}\right)\left(\frac{3}{4\pi^2}A_0{}^2A_2 + \frac{9}{16\pi^2}A_1{}^2A_2\right. \\
& \left. + \frac{3}{16\pi^2}A_2{}^3 - \frac{1}{4}A_2\right) \\
& - \cos(2\varepsilon_1 - \varepsilon_2)\left(\frac{\omega_\phi{}^2}{\omega_e}\right)\left(\frac{3}{2}l_3A_0A_1A_2 + 5l_5A_0{}^3A_1A_2\right. \\
& \left. + 5l_5A_0A_1{}^3A_2 + \frac{15}{4}l_5A_0A_1A_2{}^3 - \frac{3}{2\pi^2}F'A_0A_1A_2\right) \\
& + M'k_1\cos(3\varepsilon_1 - \varepsilon_2)\left(\frac{\omega_\phi{}^2}{\omega_e}\right)\left(\frac{3}{16\pi^2}A_1{}^2A_2\right) \\
& + M'k_2\cos(\varepsilon_2)\left(\frac{\omega_\phi{}^2}{\omega_e}\right)\left(\frac{3}{2\pi^2}A_0A_1A_2\right)
\end{aligned}
$$

$$
\begin{aligned}
0 = &-\alpha A_2 - \gamma {\omega_e}^2 \left(\frac{3}{4}{A_1}^2 A_2 + \frac{3}{2}{A_2}^3\right) \\
&- M' k_2 \sin(2\varepsilon_1 - 2\varepsilon_2)\left(\frac{{\omega_\phi}^2}{\omega_e}\right)\left(\frac{3}{32\pi^2}{A_1}^2 A_2\right) \\
&+ \sin(4\varepsilon_1 - 2\varepsilon_2)\left(\frac{{\omega_\phi}^2}{\omega_e}\right)\left(\frac{5}{64} l_5 {A_1}^4 A_2\right) \\
&- M' k_1 \sin(\varepsilon_1 - \varepsilon_2)\left(\frac{{\omega_\phi}^2}{\omega_e}\right)\left(\frac{3}{8\pi^2}{A_0}^2 A_1 + \frac{3}{32\pi^2}{A_1}^3\right. \\
&\left. + \frac{3}{32\pi^2} A_1 {A_2}^2 - \frac{1}{8} A_1\right) \\
&+ \sin(2\varepsilon_1 - \varepsilon_2)\left(\frac{{\omega_\phi}^2}{\omega_e}\right)\left(\frac{3}{8} l_3 A_0 {A_1}^2 + \frac{5}{4} l_5 {A_0}^3 {A_1}^2\right. \\
&\left. + \frac{5}{8} l_5 A_0 {A_1}^4 + \frac{15}{16} l_5 A_0 {A_1}^2 {A_2}^2 - \frac{3}{8\pi^2} F' A_0 {A_1}^2\right) \\
&- M' k_1 \sin(3\varepsilon_1 - \varepsilon_2)\left(\frac{{\omega_\phi}^2}{\omega_e}\right)\left(\frac{1}{32\pi^2}{A_1}^3\right) \\
&+ M' k_2 \sin(\varepsilon_2)\left(\frac{{\omega_\phi}^2}{\omega_e}\right)\left(\frac{1}{4\pi^2}{A_0}^3 + \frac{3}{8\pi^2} A_0 {A_1}^2\right. \\
&\left. + \frac{3}{16\pi^2} A_0 {A_2}^2 - \frac{1}{4} A_0\right)
\end{aligned}
\qquad (A.3)
$$

$$
\begin{aligned}
0 = \omega_e A_2 - \frac{1}{4}\left(\frac{\omega_\phi{}^2}{\omega_e}\right) A_2 \\
&+ F'\left(\frac{\omega_\phi{}^2}{\omega_e}\right)\left(\frac{3}{4\pi^2} A_0{}^2 A_2 + \frac{3}{8\pi^2} A_1{}^2 A_2 + \frac{3}{16\pi^2} A_2{}^3 - \frac{1}{4} A_2\right) \\
&- l_3\left(\frac{\omega_\phi{}^2}{\omega_e}\right)\left(\frac{3}{4} A_0{}^2 A_2 + \frac{3}{8} A_1{}^2 A_2 + \frac{3}{16} A_2{}^3\right) \\
&- l_5\left(\frac{\omega_\phi{}^2}{\omega_e}\right)\left(\frac{5}{4} A_0{}^4 A_2 + \frac{15}{4} A_0{}^2 A_1{}^2 A_2 + \frac{15}{32} A_1{}^4 A_2\right. \\
&\left. + \frac{15}{8} A_0{}^2 A_2{}^3 + \frac{15}{16} A_1{}^2 A_2{}^3 + \frac{5}{32} A_2{}^5\right) \\
&+ M' k_1 \cos(\varepsilon_1)\left(\frac{\omega_\phi{}^2}{\omega_e}\right)\left(\frac{3}{4\pi^2} A_0 A_1 A_2\right) \\
&+ M' k_2 \cos(2\varepsilon_1)\left(\frac{\omega_\phi{}^2}{\omega_e}\right)\left(\frac{3}{16\pi^2} A_1{}^2 A_2\right) \\
&+ M' k_2 \cos(2\varepsilon_1 - 2\varepsilon_2)\left(\frac{\omega_\phi{}^2}{\omega_e}\right)\left(\frac{3}{32\pi^2} A_1{}^2 A_2\right) \\
&- \cos(4\varepsilon_1 - 2\varepsilon_2)\left(\frac{\omega_\phi{}^2}{\omega_e}\right)\left(\frac{5}{64} l_5 A_1{}^4 A_2\right) \\
&+ M' k_1 \cos(\varepsilon_1 - \varepsilon_2)\left(\frac{\omega_\phi{}^2}{\omega_e}\right)\left(\frac{3}{8\pi^2} A_0{}^2 A_1 + \frac{3}{32\pi^2} A_1{}^3\right. \\
&\left. + \frac{9}{32\pi^2} A_1 A_2{}^2 - \frac{1}{8} A_1\right) \\
&- \cos(2\varepsilon_1 - \varepsilon_2)\left(\frac{\omega_\phi{}^2}{\omega_e}\right)\left(\frac{3}{8} l_3 A_0 A_1{}^2 + \frac{5}{4} l_5 A_0{}^3 A_1{}^2\right. \\
&\left. + \frac{5}{8} l_5 A_0 A_1{}^4 + \frac{45}{16} l_5 A_0 A_1{}^2 A_2{}^2 - \frac{3}{8\pi^2} F' A_0 A_1{}^2\right) \\
&+ M' k_1 \cos(3\varepsilon_1 - \varepsilon_2)\left(\frac{\omega_\phi{}^2}{\omega_e}\right)\left(\frac{1}{32\pi^2} A_1{}^3\right) \\
&+ M' k_2 \cos(\varepsilon_2)\left(\frac{\omega_\phi{}^2}{\omega_e}\right)\left(\frac{1}{4\pi^2} A_0{}^3 + \frac{3}{8\pi^2} A_0 A_1{}^2\right. \\
&\left. + \frac{9}{16\pi^2} A_0 A_1{}^2 - \frac{1}{4} A_0\right)
\end{aligned}
\tag{A.4}
$$

$$
\begin{aligned}
&\omega_\phi{}^2 A_0 + F'\omega_\phi{}^2\left(A_0 - \frac{1}{\pi^2}A_0{}^3 - \frac{3}{2\pi^2}A_0A_1{}^2 - \frac{3}{2\pi^2}A_0A_2{}^2\right)\\
&\quad + l_3\omega_\phi{}^2\left(A_0{}^3 + \frac{3}{2}A_0A_1{}^2 + \frac{3}{2}A_0A_2{}^2\right)\\
&\quad + l_5\omega_\phi{}^2\left(A_0{}^5 + 5A_0{}^3A_1{}^2 + \frac{15}{8}A_0A_1{}^4 + 5A_0{}^3A_2{}^2\right.\\
&\quad \left. + \frac{15}{2}A_0A_1{}^2A_2{}^2 + \frac{15}{8}A_0A_2{}^4\right)\\
&\quad - M'k_1\cos(\varepsilon_1)\,\omega_\phi{}^2\left(\frac{3}{2\pi^2}A_0{}^2A_1 + \frac{3}{8\pi^2}A_1{}^3 + \frac{3}{4\pi^2}A_1A_2{}^2\right.\\
&\quad \left. - \frac{1}{2}A_1\right) - M'k_2\cos(2\varepsilon_1)\left(\frac{3}{4\pi^2}A_0A_1{}^2\right)\\
&\quad - M'k_1\cos(\varepsilon_1-\varepsilon_2)\,\omega_\phi{}^2\left(\frac{3}{2\pi^2}A_0A_1A_2\right)\\
&\quad + \cos(2\varepsilon_1-\varepsilon_2)\,\omega_\phi{}^2\left(\frac{3}{4}l_3A_1{}^2A_2 + \frac{15}{2}l_5A_0{}^2A_1{}^2A_2\right.\\
&\quad \left. + \frac{5}{4}l_5A_1{}^4A_2 + \frac{15}{8}l_5A_1{}^2A_2{}^3 - \frac{3}{4\pi^2}F'A_1{}^2A_2\right)\\
&\quad - M'k_2\cos(\varepsilon_2)\,\omega_\phi{}^2\left(\frac{3}{2\pi^2}A_0{}^2A_2 + \frac{3}{4\pi^2}A_1{}^2A_2 + \frac{3}{8\pi^2}A_2{}^3\right.\\
&\quad \left. - \frac{1}{2}A_2\right) + \sin(2\varepsilon_1-\varepsilon_2)\left(\frac{3}{2}\gamma\omega_e{}^3A_1{}^2A_2\right) = 0
\end{aligned}
\tag{A.5}
$$

Appendix 2

The following formula can obtain the occurrence condition for fundamental parametric rolling.

$$
\begin{aligned}
&16C\omega_\phi{}^2\omega_e{}^8 + \left\{80\alpha^2C + \left(8k_1{}^2 + 2k_2{}^2\right)M'^2\omega_\phi{}^2 - 40C^2\omega_\phi{}^2\right\}\omega_\phi{}^2\omega_e{}^6\\
&\quad + \left\{64\alpha^4C + 8\alpha^2\left(k_1{}^2 + k_2{}^2\right)M'^2\omega_\phi{}^2 - 64\alpha^2C^2\omega_\phi{}^2\right.\\
&\quad + 6k_1{}^2k_2M'^3\omega_\phi{}^4 - \left(14k_1{}^2 + \frac{17}{2}k_2{}^2\right)M'^2C\omega_\phi{}^4\\
&\quad \left. + 33C^3\omega_\phi{}^4\right\}\omega_\phi{}^2\omega_e{}^4\\
&\quad + \left\{20\alpha^2C^3 - \left(4k_1{}^2 + 6k_2{}^2\right)\alpha^2M'^2C\right.\\
&\quad - \left(\frac{1}{2}k_1{}^4 - \frac{7}{8}k_1{}^2k_2{}^2 + \frac{1}{2}k_2{}^4\right)M'^4\omega_\phi{}^2\\
&\quad - \frac{9}{2}k_1{}^2k_2M'^3C\omega_\phi{}^2 + \left(7k_1{}^2 + 5k_2{}^2\right)M'^2C^2\omega_\phi{}^2\\
&\quad \left. - 10C^4\omega_\phi{}^2\right\}\omega_\phi{}^6\omega_e{}^2\\
&\quad + \frac{1}{16}\left\{\left(k_2{}^2 - 2k_1{}^2\right)k_1{}^2k_2M'^5\right.\\
&\quad + \left(3k_1{}^4 - 2k_1{}^2k_2{}^2 + 2k_2{}^4\right)M'^4C + 12k_1{}^2k_2M'^3C^2\\
&\quad \left. - \left(16k_1{}^2 + 12k_2{}^2\right)M'^2C^3 + 16C^5\right\}\omega_\phi{}^8 = 0
\end{aligned}
\tag{A.6}
$$

where $C = 1 + F'$.